

# Indoor Geomagnetic Positioning based on a Joint Algorithm of Particle Filter and Dynamic Time Warp

KaiYue Qiu

School of Geomatics and Urban Spatial Information  
Beijing University of Civil Engineering and Architecture  
Beijing 102616, China  
Email: 1181295376@qq.com

Wei Li

School of Geomatics and Urban Spatial Information  
Beijing University of Civil Engineering and Architecture  
Beijing 102616, China  
Email: 1159928759@qq.com

He Huang

School of Geomatics and Urban Spatial Information  
Beijing University of Civil Engineering and Architecture  
Beijing 102616, China  
Email: huanghe@bucea.edu.cn

DeAn Luo

School of Geomatics and Urban Spatial Information  
Beijing University of Civil Engineering and Architecture  
Beijing 102616, China  
Email: luodean@bucea.edu.cn

**Abstract**—The indoor geomagnetic field is affected by the steel structure and other ferromagnetic materials, resulting in the local anomaly of the magnetic field and the indoor geomagnetic field will be specificity. Benefit from this phenomenon, indoor magnetic positioning technology to be achieved. However, in large buildings, the specificity of geomagnetic field will be weakened, which leads to ambiguous positioning results. In response to this phenomenon, this paper presents a path matching based indoor geomagnetic positioning system, by increasing the number of matching features to solve this problem. The system combines Dynamic Time Warp (DTW) algorithm and Particle Filter (PF) algorithm to track the target in the path matching mode. Finally, Measuring robot loaded with magnetic sensor used to verify the results. The results show that the path matching has sufficient number of geomagnetic features to resolve the ambiguity of positioning results under condition of reduced specificity, and the positioning accuracy is better than 1 meter.

**Keywords**—particle filter, geomagnetic field, Dynamic Time Warp, indoor positioning Introduction

## I. INTRODUCTION

In an indoor environment such as buildings, obtaining highly accurate location information is a challenging task. Traditional methods, such as the Global Positioning System (GPS) [1], do not work inside a building due to the attenuation of satellite signals. This has prompted the development of high-precision indoor positioning systems, such as indoor positioning systems based on WiFi [2], ZigBee [3] and Radio Frequency Identification (RFID)[4]. However, when wireless technology is used to solve indoor positioning problems, the effects of physical obstacles are unavoidable, the positioning system receives the signal interference and attenuation. In addition, the above proposed indoor positioning solution also needs to solve the problems of deploying a specific device or using additional hardware in the positioning process and performing regular

maintenance of the basic device, all these come at high costs.

Thence, infrastructure-free geomagnetic positioning technology has drawn much attention. The geomagnetic field is typically used to determine the course of geomagnetic positioning equipment [5]. However, significant geomagnetic anomalies in indoor environments tend to adversely affect the accuracy of orientation estimation. Calibration is typically required, but this is not an easy task [6]. In addition, the deformation of the indoor magnetic field can be considered to be a source of information, which is caused by concrete and steel structures in the building and indoor magnetic iron equipment. The unique signature of each location can be obtained using the local anomalies of the indoor magnetic field in the room and building a geomagnetic reference map in a manner similar to fingerprinting, the geomagnetic field in the room can be time-stabilized on a time scale of several weeks or even several months [7].

As early as 2000, Suksakulchai [8] realized that magnetic field interference can be used for indoor positioning. For indoor geomagnetic localization, a known geomagnetic reference map is required. Although simultaneous positioning and mapping (SLAM) technology overcomes this requirement [9], most of related work is mainly focused on positioning, and matching algorithms typically use particle filters (PF). Seong-Eun Kim et al. [10] based on inertial sensors in smart phones, used a pedestrian dead reckoning algorithm as the motion model of the particle filter, updated the particle weights based on the total intensity of the measured magnetic field, user location be estimated within predefined search area using particle filter and used the corner between the two corridors as a position correction landmark, achieved a precision of nearly 1 meter in an experiment. In a study by Martin et al. [11], the particle filter makes use of an existing geomagnetic reference map and geomagnetic sensor measurement

information to reckon the target position. Experiments indicate that compared with only using the magnetic field strength while considering the three components of the magnetic field, will make the positioning accuracy higher, and achieved centimeter-level indoor positioning accuracy in the small area. Putta et al. [12] proposed a method of using inertial sensors, magnetic field maps and indoor maps in a particle filter-based implementation to improve the accuracy of positioning and tracking. And they added the gradient descent algorithm to correct an inaccurate estimation of user heading direction due to magnetic disturbance. Experiments using a magnetic field of three components and an indoor map achieved an average positioning accuracy of 0.75 meters with a standard deviation of 0.52 meters.

Most existing indoor geomagnetic localization based on the particle filter algorithm use each location as a matching unit. There are three combinations of location-based matching modes (using the magnetic field strength, the horizontal and vertical components, as well as x, y, and z three-axis components). Therefore, there are only three geomagnetic matching features at one point. If it only relies on the magnetic field measurements, geomagnetic matching in large areas leads to ambiguous positioning results [13]. Increasing the number of matching features is a solution. Therefore, this paper proposes a path-based matching mode; the path formed by multiple points has an enough number of matching features. Riehle et al. [14] proposed using a DTW for path matching in a one-dimensional path with a precision of nearly 1 meter. The matching algorithm proposed in this paper combines DTW with the particle filter algorithm to construct a two-dimensional path-based matching pattern, which has more advantages in matching the number of features than the common pattern based on location matching. In the indoor geomagnetic localization, path matching is actually geomagnetic sequence matching, so that it is also possible to calculate the similarity between the geomagnetic sequences as an auxiliary positioning method. Finally, the matching method proposed in this paper is evaluated through experiments.

The paper is organized as follows. Section 1 introduces related research. Section 2 introduces the indoor geomagnetic positioning system and related algorithms. Section 3 introduces the collection of experimental data and the construction of the reference map. In section 4, experimental results and their analysis are provided. Section 5 is the conclusion.

## II. GEOMAGNETIC INDOOR POSITIONING

### A. Indoor geomagnetic positioning system

The geomagnetic indoor positioning system can be divided into offline composition and online matching stages. Offline composition is the use of magnetic sensors to traverse the matching area, using collected geomagnetic data; a reference map is established using a similar "fingerprint" method. Online matching is the collection of geomagnetic data in real time during the target phase of

motion and use of the matching algorithm to make an optimal estimation with the reference map and to get the best estimate of the target position; the whole process illustrated in Figure 1. In the system, the geomagnetic matching algorithm is the core technology. The proposed algorithm in this paper is a joint algorithm that contain of DTW and PF and proposes a joint algorithm flow.

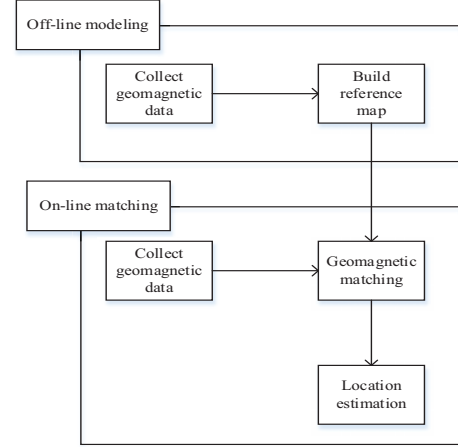


Fig. 1. Positioning the process framework

### B. Joint algorithm

The joint algorithm follows the framework of the particle filter. Firstly, a particle swarm is generated randomly in the matching region. Then, the particles move with the target according to the motion model. Thereafter, the particle path and the target path are generated after a period of moving. Finally, path matching is performed. Add DTW algorithm as match criterion in matching process, and add similarity  $\rho$  as auxiliary method. The whole joint algorithm's flow chart is in Figure 2.

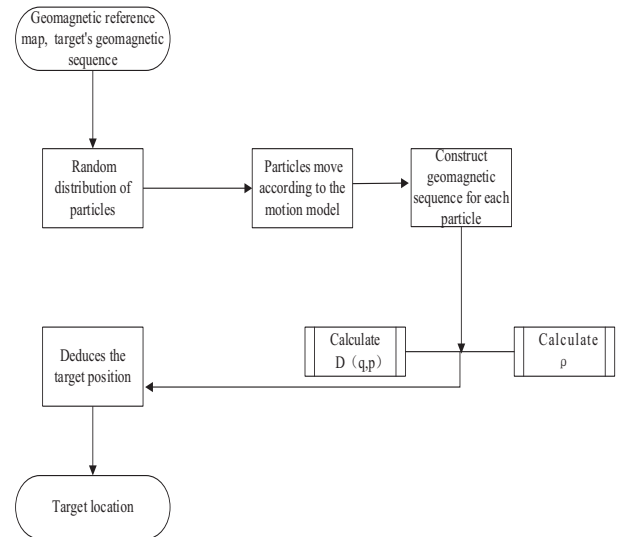


Fig. 2. Joint algorithm's flow chart

Acknowledgment: This study was supported by National Key Research and Development Program of China (No. 2017YFB0503702).

When considering path matching, one first defines the measurement distance between the field strength measured online and the reference in the fingerprint model. In general, in performing path matching (or sequence matching), collecting these geomagnetic data while walking at different speeds or at different sampling rates may result in a time-scale difference between the two sequences that render the comparison of the two sequences inaccurate. The benefit of comparing with DTW is the ability to allow two sequences be compared on different time scales. The algorithm maps a sample of one sequence to that of another in a manner that achieves a minimum of the measurement distance between the two sequences. Suppose the path traveled by the target is Q, the length  $K = q$ , the path traveled by a particle is P, and the length  $K = p$ . The metric distance of the DTW algorithm is defined as follows:

$$\begin{aligned} D(q, p) &= d(q, p) + \min[D(q-1, p), D(q, p-1), D(q-1, p-1)] \\ D(1, 1) &= d(1, 1) \end{aligned} \quad (1)$$

In Eq. (1),  $D(q, p)$  denotes the distance between paths Q and P with length q and p, respectively,  $d(q, p)$  denotes the distance measurement method of the corresponding point in the path,  $d(q, p) = \|\bullet\|$  represents the Euclidean distance. The similarity is determined by calculating Spearman's correlation coefficient, which is defined as follows:

$$\rho = \frac{\sum_{i=1}^N (x_i - \bar{x})(y_i - \bar{y})}{\sqrt{\sum_{i=1}^N (x_i - \bar{x})^2 \sum_{i=1}^N (y_i - \bar{y})^2}} \quad (2)$$

where  $x_i$  and  $y_i$  represent i-th data of target sequence and a particle sequence, respectively,  $\bar{x}$  and  $\bar{y}$  represent the average of the two sequence data respectively, and the coefficient requires that the lengths of the two sequences be the same.

In general, the particle filter uses the Monte Carlo Localization (MCL) method to approximate the posterior probability distribution  $p(x_t | z_t)$  when it is too complex to be directly sampled, but the prior probability density  $p(x_t | x_{t-1}^i)$  can be sampled, and the measurement density  $p(z_t | x_t^i)$  can be evaluated. The principle is to use the state of the particle as prior probability and the target observation value as a parameter to match the reference value corresponding to the position of the particle. Finally, the maximum likelihood estimation of the target, i.e. the posterior probability, is deduced.

$$\begin{aligned} p(\bar{x}_t | z_{t-1}) &\sim p(x_t | x_t^i) \\ p(x_t | z_t) &\sim \frac{p(\bar{x}_t | z_{t-1}) p(z_t | x_t^i)}{c} \end{aligned} \quad (3)$$

Where,  $x_t$  represents the target positioning,  $\bar{x}_t$  indicates the predicted location of target  $x_t^i$  represents the particle's positioning,  $z_t$  is the observation,  $t$  represents continuance time, and  $c$  is a normalization constant. The entire particle filtering process consists of three steps, namely forecasting, updating, and resampling. It first extracts a set of N particle sample sets from the prior probability density. The weights  $w^i$  are then generated for each particle based on the likelihood function  $p(z_t | x_t^i)$ , and the particle weights are normalized prior to resampling so that the sum of weights is one. The basic idea of resampling is to remove the less-weighted particles and duplicate the heavily-weighted particles. In the two-dimensional positioning, the pedestrian trajectory is provided as the basis for the motion model of the particle filter algorithm. The model is as follow:

$$x_t^i = x_{t-1}^i + l * H \quad (4)$$

Where  $l \sim U(0, L)$ ,  $U(0, L)$  obeys a uniform distribution,  $L$  is the moving distance, and

$$H = \begin{bmatrix} \sin \theta & 0 \\ 0 & \cos \theta \end{bmatrix} \quad (5)$$

In Eq. 5,  $\theta$  is the moving direction. The likelihood function  $p(z_t | x_t^i)$  is based on the single variable Gaussian probability density function, which is given by

$$p(z_t | x_t^i) = \frac{1}{\sigma_r \sqrt{2\pi}} \exp\left[-\frac{(z_t - f(x_t^i))^2}{2\sigma_r^2}\right] \quad (6)$$

Where  $\sigma_r$  is the covariance of the observation  $z_t$ . The function  $f(x_t)$  returns the magnetic field intensity of the position  $x_t^i$  in the fingerprint model. Finally, the position  $\hat{x}_t$  of the target is estimated based on the weight  $w$  of the sample particles and which is given by

$$\hat{x}_t = \sum_{i=1}^N w_t^i x_t^i \quad (7)$$

Finally, the positioning error is given by Eq. 8,

$$err = \sqrt{(x_t - \hat{x}_t)^2} \quad (8)$$

It is different from the general particle filter because of the following reasons:

a) It increases the number of matching elements and improves the matching accuracy.

b) It uses the DTW algorithm, the distance between particle and the target instead of the particle weight without resampling.

c) It reduces the need for the number of particle swarms.

d) It uses geomagnetic sequence similarity to aid location.

### III. EXPERIMENTAL DATA COLLECTION AND REFERENCE MAP CONSTRUCTION

The experimental site is the corridor on the second floor of the School of Geomatics and Urban Spatial Informatics, Beijing University of Civil Engineering and Architecture. It is 68 meters long and 1.8 meters wide. The plan is illustrated in Figure 3. The premise of studying geomagnetic indoor positioning is to construct the geomagnetic reference map. In this paper, the collected geomagnetic data of the second floor corridor are used to construct a reference map using the fingerprint mode.

To collect indoor geomagnetic data quickly, our team (the Urban Surveying and Mapping Institute) developed a measurement robot that is equipped with a HMC5983 geomagnetic sensor and a loading location of 1.3 meters from the ground, to avoid the robot's influence on itself, as illustrated in Figure 4 [15]. The HMC5983 is small, with automatic offset compensation and temperature compensation and carries I2C or SPI digital interface, the maximum output power of 220 Hz, the heading angle accuracy of 1-2 degrees. we use the magnetic field intensity  $\|m\|$  as a matching feature because the magnetic field intensity is a rotation invariant, which avoids the influence of a slight jitter on the experiment during the movement of the device;  $\|m\|$  is defined as follows.

$$\|m\| = \sqrt{m_x^2 + m_y^2 + m_z^2} \quad (9)$$

In the corridor, we collected geomagnetic data in the middle of the corridor along the 4 lines, which were 60 cm apart from each other by the measurement robot.

The robot step size is 0.2 m, and the magnetic field is measured every 25 Hz to generate a three-dimensional vector  $m = [m_x, m_y, m_z]$ , in units of  $\mu T$ . The acquisition time of each point is 10 seconds.

The collected reference geomagnetic data were processed by the Kriging interpolation and assigned to the grid coordinates. The geomagnetic reference map is provided in Figure 5. As can be seen in the figure, under the influence of the reinforced concrete structure of the building, the geomagnetic disturbance of the corridor changes with the change of the space position and can thus be used for indoor positioning. The circle in the figure represents the similar phenomenon of geomagnetic intensity, which leads to the weakening of the geomagnetic specificity in the interior and the introduction of errors in the positioning result.

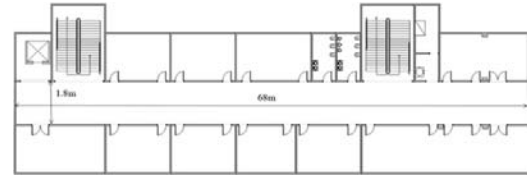


Fig.3. The corridor plan

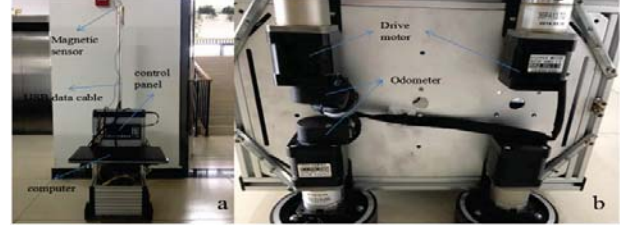


Fig. 4. Measurement robot structure

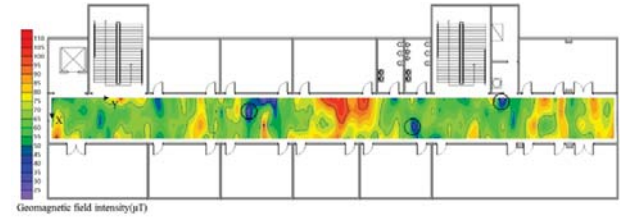


Fig. 5. The geomagnetic reference map

### IV. EXPERIMENTAL RESULTS AND ANALYSIS

In this paper, the influence of the number of particles  $N$  and the path length  $K$  on the positioning accuracy was first analyzed under the same distribution of sampled particles. The measurement robot moves linearly 15 times along the Y axis, starting from a random point (1.2, 15.4), and the step length  $L$  was set at 0.6 m. The geomagnetic data were acquired, and 15 locations were obtained. There were 14 kinds of path length, as illustrated in Figure 6. The path length between two adjacent points was 1 (which represents 0.6 m), as illustrated in the figure. In addition, path-based matching could only be executed from location 2, and at each location, the number of features used was equal to the number of location.

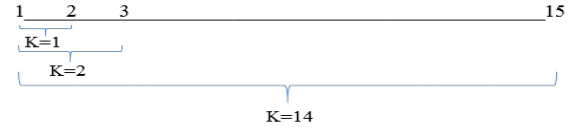


Fig. 6. The relationship between locations and sequence length  $K$

After the geomagnetic data was collected, it was matched with the geomagnetic reference map using the joint algorithm. Particle distribution in the particle filter algorithm was randomly distributed, the number of matching was set at 300 times, and the joint algorithm was implemented by the MatLab software. The results are presented in Figures 7 and 8. The figures illustrate the



positioning error (average positioning error) and the percentage of error (PE), respectively, as functions of the number of particles.

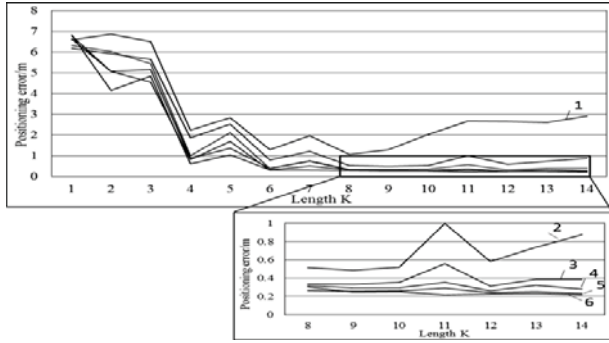


Fig.7. The positioning error results for different numbers of particles (The numbers represent the units of 100 particles, which means that 1 represents 100; the small figure illustrates partial enlargement.)

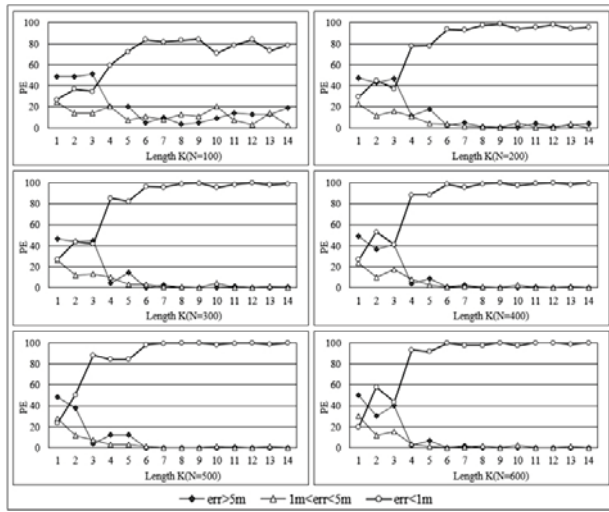


Fig. 8. Percentage of error (PE)

It can be seen in Figure 7 that when the particles are sparse, unstable positioning occurs, for example,  $N = 100$  and  $N = 200$ , which are related to the particle distribution. If the randomly distributed position of particles is very close to the target, it leads to high-precision positioning results. When  $N$  is less than 500, there are fluctuations when  $K = 5$  or 7, fluctuations are related to the choice of this path; however, this does not affect the overall positioning result of the experiment that when  $K$  is greater than 9, the positioning error is below or close to 1 m (except  $N = 100$ ).

A sufficient number of particles can ensure that the particles are densely distributed, so there is a large probability of particles to be randomly distributed around the target, resulting in a high probability of high-precision positioning results, as illustrated in Figure 8. As can be seen in Figure 8, when the path length is constant, the percentage of error ( $<1$  m) increases as the number of particles

increases; When  $N > 300$ , the variation trend of the percentage of each error interval (with the change of the  $K$  value) basically remains the same.

Overall, when  $N$  is greater than 100, the overall positioning accuracy increases with  $K$ , especially when  $N$  is greater than 300, and the positioning accuracy is better than 1 meter if the path length  $K$  exceeds 7. At the same time, considering that if  $N$  is too large it brings a big burden on the operation of the algorithm, the optimal experimental parameters at  $N = 400$  were determined.

In traditional particle filter, due to the SIR algorithm, the positioning results converge, as illustrated in Figure 9. It can be seen in the figure that the result of using a single-location on the same path with particle filter starts to converge at roughly location 5. However, the convergence result is ambiguous; in the random match of 20 times, the maximum convergence error can be close to 20 m, and the minimum convergence error can be less than 1 m. Then we perform the same experiment 300 times, and the percentage of each positioning error range at point 15 was obtained at the same time with the proposed method for comparison, as illustrated in Figure 10. This figure fully illustrates single-location matching model, which leads to the stability of particle filters being decreased. Such stability is not enough for indoor positioning, compared with that of the proposed method, which has good stability and positioning accuracy within 1 m close to 100%.

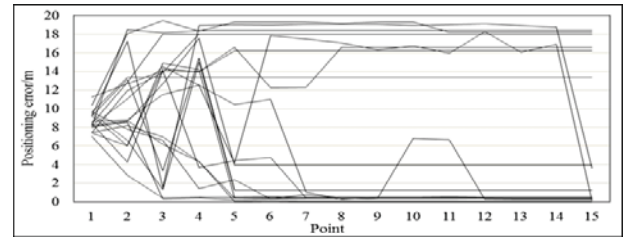


Fig.9.Single location positioning based on particle filter for the same path ( $N = 400$ )

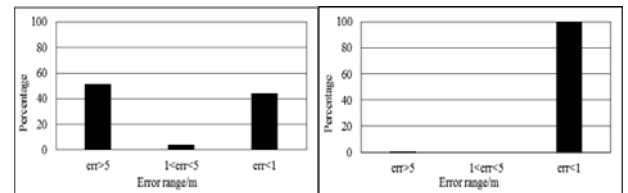


Fig.10. Particle filter and joint algorithm error proportioning diagram ( $N = 400$ ) (The left-hand figure is based on single-location matching, and the right-hand figure is based on path matching.)

The method proposed in this paper includes the sequence similarity that is as an auxiliary mean. To verify the effectiveness of the auxiliary means. We performed a comparative experiment ( $N=400$ ); the results are illustrated in Figure 11. As can be seen in the figure, From  $K = 1$  to  $K = 14$  (location 2 to location 15), the use of geomagnetic sequence similarity as an auxiliary means can improve the

positioning accuracy of the path matching process; the shorter the path, the more obvious the effect.

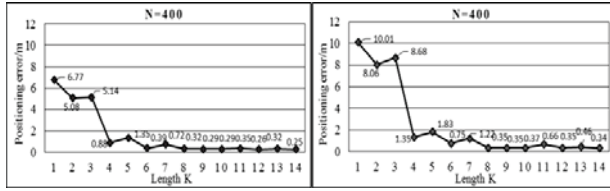


Fig. 11.  $N = 400$  comparison of positioning results (The figure on the left illustrates the addition of means, and the figure on the right illustrates no addition of means.)

To verify the robustness of the method, also randomly from four different locations (a total of five) to collect a geomagnetic sequence, the step length  $L$  was unchanged. The number of particles  $N$  was set at 400, including two right-angle turning paths; the result is illustrated in Figure 12. In the figure, 1, 2 and 3 represent the straight-line path, while 4 and 5 represent the path including the right-angle. Obviously, when  $K$  was greater than 9, the optimal positioning accuracy was within 1 m; there is no sudden sharp increase in the positioning error, which indicates that the proposed technique is reliable and has good robustness. This also proves that the choice of the path does not affect the overall positioning accuracy as mentioned above. In addition, the experiment in this paper is to verify the plausibility of indoor geomagnetic localization based on the path mode and to obtain the positioning accuracy of the system. Therefore, the measurement robot's movement step and heading angle belong to manual control.

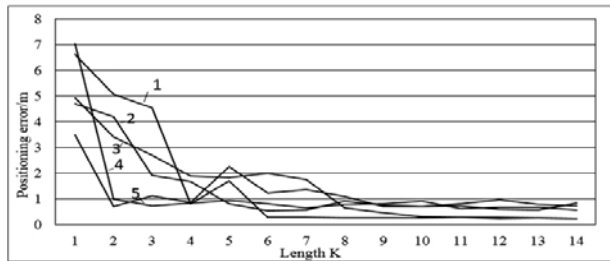


Figure 12. Comparison of positioning errors of different paths

## V. CONCLUSION

In the development of location-based services, the premise is indoor positioning. Methods based on geomagnetic localization have received widespread attention because they require no other infrastructure investment. However, in large buildings, the specificity of the geomagnetic field is weakened. The general location based method based on particle filter is likely to result in ambiguous positioning results. In this paper, a new geomagnetic indoor positioning technology is proposed. There are two innovations in this technology:

a) The proposed a joint algorithm based on particle filter and DTW as well as

b) A new geomagnetic localization mode based on path matching.

Path-based matching is actually based on geomagnetic sequence matching, so sequence similarity is added as an adjunct, and later experiments also prove the effectiveness of the assistive approach. Finally, the experimental results indicate that compared with the traditional geomagnetic indoor positioning method based on the particle filter algorithm, the proposed method effectively restrains the localization ambiguity problem. When the path length and the number of particles are enough ( $K \geq 9$  and  $N \geq 400$ ), the overall positioning accuracy is higher than 1 m, and the probability of positioning accuracy lower than 1 m is close to 100%, which indicates the excellent stability and reliability performance.

## REFERENCES

- [1] Misra, P.; Enge, P. Special issue on global positioning system. IEEE Proc. 1999, 87, 3–15.
- [2] Garcia-Valverde, T.; Garcia-Sola, A.; Hagraas, H.; Dooley, J.A.; Callaghan, V.; Botia, J.A. A Fuzzy Logic-Based System for Indoor Localization Using WiFi in Ambient Intelligent Environments. IEEE Trans. Fuzzy Syst. 2013, 21, 702–718.
- [3] Luoh, L. ZigBee-based intelligent indoor positioning system soft computing. Soft Comput. 2013, 18, 443–456.
- [4] Ni, L.; Liu, Y.; Lau, Y.; Patil, A. LANDMARC: Indoor location sensing using active RFID. Wirel. Netw. 2004, 10, 701–710.
- [5] Skvortzov, V.Y.; Lee, H.K.; Bang, S.W. & Lee, Y.B. 2007, Application of electronic compass for mobile robot in an indoor environment, Robotics and Automation, 2007 IEEE International Conference on, pp2963-2970.
- [6] Afzal, M.H.; Renaudin, V. & Lachapelle, G. 2011, Multi-magnetometer based perturbation mitigation for indoor orientation estimation, NAVIGATION, vol. 58, no. 4.
- [7] B. Li, T. Gallagher, A. G. Dempster, and C. Rizos, "How feasible is the use of magnetic field alone for indoor positioning?," 2012 Int. Conf. Indoor Position. Indoor Navig. IPIN 2012 - Conf. Proc., no. November, pp. 1–9, 2012.
- [8] S. Suksakulchai, S. Thongchai, D. M. Wilkes, and K. Kawamura, "Mobile robot localization using an electronic compass for corridor environment," IEEE Int. Conf. Syst. Man, Cybern., vol. 5, pp. 3354–3359, 2000.
- [9] I. Vallivaara, J. Haverinen, A. Kempainen, and J. Roning, "Simultaneous localization and mapping using ambient magnetic field," Proc IEEE Intern. Conf Multisens. Fusion Integr. Intell. Syst., pp. 14–19, 2010.
- [10] S. E. Kim, Y. Kim, J. Yoon, and E. S. Kim, "Indoor positioning system using geomagnetic anomalies for smartphones," 2012 Int. Conf. Indoor Position. Indoor Navig. IPIN 2012 - Conf. Proc., no. November, 2012.
- [11] M. Frassl, M. Angermann, M. Lichtenstern, P. Robertson, B. J. Julian, and M. Doniec, "Magnetic maps of indoor environments for precise localization of legged and non-legged locomotion," in IEEE International Conference on Intelligent Robots and Systems, 2013, pp. 913–920.
- [12] R. Putta, M. Misra, and D. Kapoor, "Smartphone based indoor tracking using magnetic and indoor maps," 2015 IEEE 10th Int. Conf. Intell. Sensors, Sens. Networks Inf. Process. ISSNIP 2015, no. April, pp. 7–9, 2015.
- [13] B. Li, T. Gallagher, C. Rizos, and A. G. Dempster, "Using geomagnetic field for indoor positioning," J. Appl. Geod., vol. 7, no. 4, pp. 299–308, 2013.
- [14] T. H. Riehle, S. M. Anderson, P. A. Lichter, J. P. Condon, S. I. Sheikh, and D. S. Hedin, "Indoor waypoint navigation via magnetic anomalies," Proc. Annu. Int. Conf. IEEE Eng. Med. Biol. Soc. EMBS, pp. 5315–5318, 2011.

- [15] H. Huang, Y. Zhao, C. L. Wang, et al., "Design of the Acquisition System of Indoor Positioning Reference Map Based on Magnetic Field Data," *Bulletin of Surveying and Mapping*, vol.2, pp.54-59,2017.